ISSN: 2993-3617

Research Article

Journal of Oil and Gas Research Reviews

A Cartographic and Remote Sensing Comparison of Zabadani Geological Maps: from Stratigraphic Synthesis to Structural Cartography

Jean A. Doumit*

Lebanese University, Faculty of Letters and Human Sciences, Department of Geography, Geospatial lab, Lebanon

***Corresponding Author**
Jean A. Doumit, Lebanese University, Faculty of Letters and Human Sciences, Department of Geography, Lebanon.

Submitted: 2026, May 26 **Accepted:** 2026, Jun 30; **Published:** 2026, Jul 10

Citation: Doumit, J. A. (2026). A Cartographic and Remote Sensing Comparison of Zabadani Geological Maps: from Stratigraphic Synthesis to Structural Cartography. *J Oil Gas Res Rev, 6*(2), 01-12.

Abstract

This study reconstructs and compares two major mid-20th-century geological maps of the tectonically complex Zabadani area (at a 1:50,000 scale) to assess their spatial and lithologic consistency. Modern GIS workflows allow for scanning, georeferencing, digitizing, and harmonizing using a unique historical sheet legend by Louis Dubertret and Vladimir Ponikarov. The results of the overlay analysis show that spatial differences accounting for about 20% of the study area are located along the fuzzy boundaries between the Lower Cretaceous and Upper Jurassic sequences. While Dubertret's regional chronostratigraphic continuity, Ponikarov's structural approach captures much more lithomechanical detail and fault density. To address these inconsistencies, we applied zonal statistics on NASA's EMIT Level 2B mineral-fraction products (60 m resolution). Both maps show the regional carbonate platform. EMIT images show a diverse mineral landscape at the subpixel scale, including halloysite, Clinochlore, hectorite, muscovite, and dickite. This hyperspectral fingerprinting confirms Ponikarov's more detailed stratigraphic subdivisions in a direct way. This integrated workflow ultimately demonstrates that combining legacy cartography with advanced imaging spectroscopy effectively isolates real ground-level mineralogical variations from cartographic artifacts, providing an empirical roadmap for future field verification.

Keywords: Geology Mapping, Remote Sensing, EMIT, Ponikarov, Dubertret

1. Introduction

At its heart, geology concerns the distribution of rocks and the evolution of the Earth's crust, but in areas of complex tectonics, this is especially challenging. This is primarily accomplished through geological maps, which are essential for natural resource exploration, infrastructure development and hazard assessment [1,2]. In areas such as Lebanon and Syria, where complex tectonic and stratigraphic relationships are found, the interpretation of geological maps is closely tied to the mapping methods and objectives [3,4]. An illustration of this development is the evolution of geological mapping in Lebanon. The first detailed stratigraphic synthesis of the region was produced by Louis Dubertret in the mid-20th century; his maps emphasized lithostratigraphic succession and established key geological terminology, providing a consistent framework for the Jurassic and Cretaceous carbonate formations of the area [3,5]. Later, surveys under the Soviet Union, especially those of Vladimir Pavlovich Ponikarov, applied a structurally oriented mapping approach. These maps focused on faults, fracture networks and rock-mechanical properties, providing a clearer view of structural complexity [4,6]. Both mapping approaches cover the same geological formations, with similar focus and presentation, indicating the transition in geological cartography from stratigraphic synthesis to application-oriented structural mapping [7]. Advances in Geographic Information Systems (GIS) and remote sensing now allow for the digitization, georeferencing and quantitative comparison of historic maps with satellite-based lithological data [8,9]. The Earth Surface Mineral Dust Source Investigation (EMIT) imagery mission is designed to automate mapping and provide independent validation of geological interpretations. The Zabadani region of the Anti-Lebanon Mountains, on the Lebanon-Syria border, provides an excellent test case for evaluating these approaches. The complex sequences of Jurassic and Cretaceous carbonate formations were mapped at comparable scales by both Dubertret and Ponikarov,

providing a unique opportunity to compare mapping techniques and assess spatial accuracy [3,4]. The geological knowledge of the Zabadani (Zebdani) basin in south-western Syria has been established by two major mapping traditions. In the 1940s-1950s, Louis Dubertret directed the French surveys that resulted in the 1:50,000 "Feuille de Zebdani" (emphasizing structural geology and regional stratigraphy). Dubertret mapped major faults and folds and interpreted the Zebdani plain as a fault-bounded basin within the Anti-Lebanon structural system. His detailed field observations served as the baseline for later studies, including simplified cross Sections and hydrogeological assessments [10-12].

In the 1960s, Ponikarov coordinated the Syrian national geological survey that produced a similar 1:50,000 Zabadani sheet with explanatory notes. Ponikarov, in contrast to Dubertret, used a standardized coded legend and combined geological mapping with assessments of mineral and groundwater resources. His work introduced new tectonic ideas and emphasized the importance of Cenozoic and Quaternary units relevant to hydrogeology and geophysical interpretation, which became the operational standard for resource assessment in the Syrian basins [10,13,14].

Both maps are at the same scale and cover the same area but differ in focus and methodology. Dubertret is qualitative, emphasizing structural and stratigraphic detail, while Ponikarov is systematic and resource-oriented in its stratigraphy. Dubertret is primarily used for historical structural context, and Ponikarov for hydrogeological modeling and groundwater management. Current research often uses both sources [10,12-15]. These dual legacies illustrate the complementary role of both mapping programs and form the basis of modern geological and hydrogeological studies in the Zabadani basin. The methodological approach, focus, and cartographic standards of historical geological maps differ, making them difficult to integrate into modern GIS frameworks and limiting their potential for validation using modern geospatial techniques [16]. The aim of this study is to (1) compare the geological maps of Dubertret and Ponikarov to assess methodological and spatial differences (2) quantify spatial discrepancies using GIS tools (3) assess the correspondence between mapped units and classifications derived from multispectral satellite imagery and (4) assess the potential of remote sensing to complement and validate historical geological mapping. Historical maps can be georeferenced and digitized in a meaningful way for comparison in a GIS environment [17]. Remote sensing can accurately determine lithologic and structural features and provide independent validation of historical maps [9,18]. Integrating historical mapping with remote sensing will identify areas of concordance and discrepancy, guiding future field verification [8,19].

EMIT is considered a major advancement in geological mapping because it uses imaging spectroscopy (hyperspectral remote sensing) rather than the broader multispectral bands of sensors such as Landsat and Sentinel-2. In contrast to traditional multispectral sensors (e.g., Landsat and Sentinel-2), EMIT's hyperspectral imaging provides detailed mineralogical discrimination through contiguous, narrow spectral bands, greatly enhancing lithological differentiation, alteration mapping, and structural interpretation for geological cartography.

The extreme tectonic deformation associated with the Dead Sea Transform system, particularly along major fault corridors such as the Serghaya Fault, adds to the geological complexity of the study area. This long-lived strike-slip and transpressional activity has extensively sheared, offset, and locally obscured lithologic boundaries, producing highly discontinuous, structurally reworked contacts. In many localities, primary stratigraphic relations are strongly overprinted or not directly observable in the field owing to faulting, fracturing, and associated weathering. Hence, traditional field-based mapping by itself is inadequate for reliable boundary tracing and unit correlation. In this sense, validation based on remote sensing is a key complementary approach, enabling continuous spatial observation and objective spectral discrimination of lithologic units in structurally complex and partially inaccessible terrains.

Knowledge of rock distributions and the evolution of the Earth's crust is fundamental to geology, yet particularly challenging in regions of complex tectonics. This knowledge is primarily conveyed through geological maps, which are essential for natural resource exploration, infrastructure development, and hazard assessment [1,2]. In areas such as Lebanon and Syria, where complex tectonic and stratigraphic relationships are found, the interpretation of geological maps is closely tied to mapping methods and objectives [3,4]. The development of geological mapping in Lebanon illustrates this progression. The first detailed stratigraphic synthesis of the region was produced by Louis Dubertret in the mid-20th century; his maps emphasized lithostratigraphic succession and established key geological terminology, providing a consistent framework for the area's Jurassic and Cretaceous carbonate formations [3,5]. Later, Soviet surveys, especially those of Vladimir Pavlovich Ponikarov, applied a structurally oriented mapping approach. These maps focused on faults, fracture networks, and rock-mechanical properties, providing a clearer view of structural complexity [4,6]. Both mapping approaches cover the same geological formations, with similar focus and presentation, indicating a transition in geological cartography from stratigraphic synthesis to application-oriented structural mapping [7]. Advances in Geographic Information Systems (GIS) and remote sensing now enable the digitization, georeferencing, and quantitative comparison of historic maps with satellite-based lithological data [8,9]. The Earth Surface Mineral Dust Source Investigation (EMIT) imagery mission is designed to automate mapping and provide independent validation of geological interpretations. The Zabadani region of the Anti-Lebanon Mountains, on the Lebanon-Syria border, provides an excellent test case for evaluating these approaches. The complex sequences of Jurassic and Cretaceous carbonate formations were mapped at comparable scales by both Dubertret and Ponikarov, providing a unique opportunity to compare mapping techniques and assess spatial accuracy [4,5].

The geological knowledge of the Zabadani (Zebdani) basin in

southwestern Syria has been established by two major mapping traditions. In the 1940s-1950s, Louis Dubertret directed the French surveys that produced the 1:50,000 "Feuille de Zebdani" (emphasizing structural geology and regional stratigraphy). Dubertret compiled the main faults and folds and interpreted the Zebdani plain as a faulted basin within the structural domain of the Anti-Lebanon. His detailed field observations formed the foundation for later simplified cross sections and hydrogeological calculations, providing an important baseline for subsequent studies [10-12]. In the 1960s, Ponikarov headed the Syrian national geological survey, which compiled a similar 1:50,000 Zabadani sheet with explanatory notes. Unlike Dubertret, Ponikarov applied a standardized coded legend, combining geological mapping with assessments of mineral and groundwater resources. His work incorporated newer tectonic concepts and focused on Cenozoic and Quaternary units important for hydrogeology and geophysical interpretation, thereby setting the operational standard for resource assessment in the Syrian basins [10,13,14].

Both maps are drawn on the same scale and cover the same area but differ in focus and method. Dubertret's map provides qualitative structural and stratigraphic details, whereas Ponikarov's focuses on systematic, resource-oriented stratigraphy. Dubertret is primarily used for historical structural context, whereas Ponikarov is used for hydrogeological modeling and groundwater management. Current research often uses both sources [10,12-15]. These dual legacies illustrate the complementary role of both mapping programs and form the basis of modern geological and hydrogeological studies in the Zabadani basin. The methodological approach, focus, and cartographic standards of historical geological maps differ, making it difficult to integrate them into modern GIS frameworks and limiting their potential for validation using modern geospatial techniques [16]. The aim of this study is to (1) compare the geological maps of Dubertret and Ponikarov to assess methodological and spatial differences (2) quantify spatial discrepancies using GIS tools (3) assess the correspondence between mapped units and classifications derived from multispectral satellite imagery and (4) assess the potential of remote sensing to complement and validate historical geological mapping. Historical maps can be georeferenced and digitized in a meaningful way for comparison in a GIS environment [17]. Remote sensing can accurately determine lithologic and structural features and provide independent validation of historical maps [9,18]. Integrating historical mapping with remote sensing will identify areas of concordance and discrepancy, guiding future field verification [8,9].

EMIT is considered a major advancement in geological mapping because it uses imaging spectroscopy (hyperspectral remote sensing) rather than the broader multispectral bands of sensors such as Landsat and Sentinel-2. In contrast to traditional multispectral sensors (e.g., Landsat and Sentinel-2), EMIT's hyperspectral imaging provides detailed mineralogical discrimination through contiguous, narrow spectral bands, greatly enhancing lithologic differentiation, alteration mapping, and structural interpretation for geological cartography. The extreme tectonic deformation associated with the Dead Sea Transform system, particularly along major fault corridors such as the Serghaya Fault, adds to the geological complexity of the study area. This long-lived strike-slip and transpressional activity has extensively sheared, offset, and locally obscured lithologic boundaries, producing highly discontinuous, structurally reworked contacts. In many localities, primary stratigraphic relations are strongly overprinted or not directly observable in the field owing to faulting, fracturing, and associated weathering. Therefore, conventional field-based mapping alone is inadequate for reliably tracing boundaries and correlating map units. In this context, remote-sensing-based validation is a critical complementary approach, providing spatially continuous observations and objective spectral discrimination of lithologic units in structurally complex and partially inaccessible terrains.

2. Materials and Methods

The study area is in the Zabadani basin within the Anti-Lebanon mountain range along the Lebanon-Syria border and covers 644 sq. km (Figure 1). The area is marked by complex topography and structural deformation related to the tectonic evolution of the Levant fault system. The stratigraphic succession exposed in the area comprises Jurassic carbonate platforms, Lower Cretaceous sandstones and limestones, Upper Cretaceous Chalky Limestones, Paleogene limestones and marls, Neogene sediments, and Quaternary deposits.

These formations are affected by folding, faulting, and fracturing associated with regional tectonic deformation.

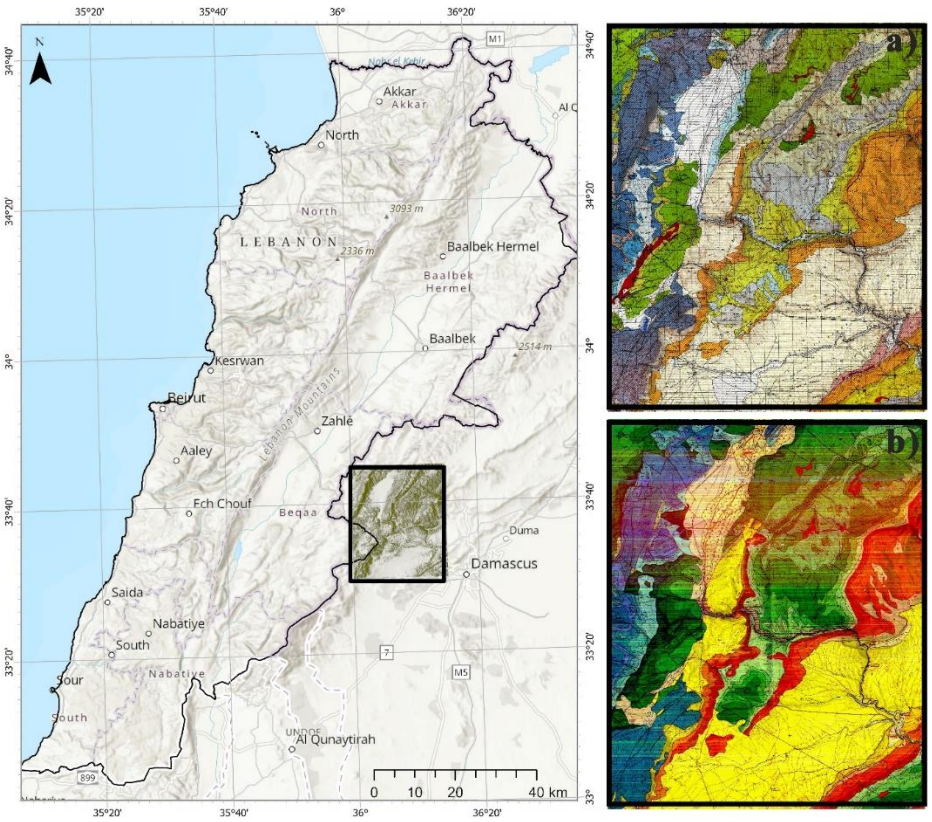

Figure 1: Study Area Location: (A) Dubertret Geological Map; (B) Ponikarov Geological Map

The cartographic data consisted of paper geological maps by Dubertret and Ponikarov (1:50,000 scale). The geological map was initially digitized using the workflow illustrated in Figure 1: paper maps were scanned at 500 dpi. The geological paper maps were first georeferenced in the Lambert Conformal Conic projection and then digitized in the UTM Zone 36N coordinate system. To maintain spatial consistency and reduce cartographic distortion during transformation, all datasets were unified to the WGS 84 datum. Legacy map grids referenced to local or regional datums (e.g., Deir ez-Zor / Syria local grid) were transformed to WGS 84 using standard Helmert transformation parameters prior to re-projection, where applicable. This workflow ensured geometric compatibility between historical cartographic products and modern satellite-based datasets, thereby reducing positional bias during digitization and subsequent spatial analysis.

The acquired geological database is not the same as Table 1, since the two maps employ different stratigraphic classification systems. The legends were unified to allow direct comparison. Examples of unit harmonization include merging Lower Cretaceous units C2a, C2b1, and C2b2 into C2 to conform to Dubertret; merging Jurassic units J4–6 into J4; and renaming Ponikarov's C4a to C4 to conform to Dubertret. Furthermore, C3-4 was merged with C3 (Dubertret units). This standardization enabled spatial comparison of geological units between the two datasets.

	PONIKAROV	DUBERTRET	Unification	Descriptions as per PONIKAROV
QUATERNARY	β	β	β	Small cutted subvolcanic basaltoid bodies
	Q4	q	q	Recent Loams, sands, pebbles
	Q3-4	q	q	PLEISTOCENE, Upper Quaternary - Recent undifferentiated. Conglomerates, pebbles, loams, sandy loams
	Q3	q	q	PLEISTOCENE, Upper Quaternary. Conglomerate, conglomerates, pebbles
	Q1	q	q	PLEISTOCENE, Lower Quaternary. Calcareous luffs, limestones, gravels
NEO-GENE	N2a	N2	N2	Pliocene, lower part. Conglomerates, sandstones, gravels, limestones
	βN21	βn	βn	Middle Miocene, Clays, sands, sandstones, pebbles, limestones.
	N21	N1	N1	Basalts

PALEOGENE	Pg32	E2	E	Upper Eocene Limestones
	Pg22-3	E2	E	Middle-Upper Eocene undifferentiated. Limestones
	Pg22	E2	E	Middle Eocene. Limestones, marls, clayey marls, and conglomerates
	Pg12p	E1	E	Lower Eocene Subzone Acarinina pentacamerata Limestones, flints, conglomerates
	Pg1-Pg12ar	E1	E	Paleocene - Lower Eocene, subzone Globorotalia aragonensis Marls, clayey marls
UPPER CRETACEOUS	Cr2m-d	C6	C6	Maestrichtian - Danlan undifferentiated. Limestones, marls, calcareous clays
	Cr2cp	C6	C6	Campanian. Limestones, flints
	Cr2cnb-st	C6	C6	Coniacian. upper part - Santonian undifferentiated Chalky limestones, marls
	Cr2cna	C6	C6	Coniacian, lower part. Limestones, calcareous dolomites, dolomites
	Cr2t1	C5	C5	Lower Turanian. Limestones, marly limestones, marls
	Cr2cm*b*	C4b, C'4	C4	Cenomanian, upper part. Dolomites, calcareous dolomites
	Cr2cm*a*	C4a	C4	Cenomanian, lower part. Limestones, clayey limestones, marls
LOWER CRETACEOUS	Cr1al	C3	C3	Albian Limestones, marly limestones, marls
	Cr1ap2*b*	C2b2	C2	Upper Aptian, upper part. Sandstones
	Cr1ap2*a*	C2b1	C2	Upper Aptian, lower part (La Muraille de Blanche). Limestones
	Cr1a.ap2	C1, C2a	C1	Pre-Upper Aptian deposits (Grés de base), Sandstones, clays.lignites. brown ironstones
	βCr1a.ap2	βC1	βC1	Basalts
JURASSIC	J3t	J7	J7	Titonian Limestones, marly clays
	J3km	J6	J6	Kimmeridgian. Limestones
	J3ox2	J5	J5	Upper Oxfordian. Marls, clayey limestones, limestones
	J3ox1	J5	J5	Lower Oxfordian Limestones
	J3cl	J4	J4	Callovian. Limestones, dolomitic limestones, and calcareous dolomites
	J2bt	J4	J4	Middle Jurassic Bathonian. Limestones, marls

Table 1: Unification of Geological Terms and their Descriptions

GIS spatial analysis was used to examine the distribution of geological units and identify differences between the two maps. The procedure included determining the surface area of each lithological unit (Table 2), superimposing the two geological maps, and extracting polygons that represent zones of disagreement (Figure 3). The NASA Earth Surface Mineral Dust Source Investigation (EMIT) mission launched in 2022 and is currently operated from the International Space Station to provide high-fidelity imaging spectroscopy in the visible to shortwave infrared (VSWIR; 380–2500 nm) at a spatial resolution of 60 m [20]. Its primary scientific objective is to characterize the mineral composition of Earth's arid dust-source regions to reduce uncertainties in radiative forcing models, with a focus on the spectral signatures of 10 key minerals, including hematite, goethite, and kaolinite [21]. In addition to its primary role in Earth System Models (ESMs), EMIT's state-of-the-art Dyson spectrometer design enables accurate retrieval of surface reflectance (Level 2A) and mineral abundance (Level 2B), and facilitates detection of greenhouse gas super-emitters, e.g., methane and carbon dioxide, by means of high-resolution absorption analysis [22,23].

The Level 2B (L2B) product generally includes a Mineral Fraction layer. This layer is a stacked raster with each band representing a different mineral. NASA uses TETRACORDER or similar linear spectral unmixing algorithms that compare the EMIT spectral signature with the USGS Spectral Library to determine the mineral combination that best matches the observed reflectance.

L2B data have been processed to include atmospheric correction and spectral unmixing, yielding estimates of mineral fractional abundances. Therefore, level 2B data provide the expected percentage of a given mineral within each 60 m pixel, making comparisons with geological maps more robust. EMIT hyperspectral imagery offers high-resolution, quantitative validation of existing geological datasets. This method is especially valuable for detecting discrepancies between mapped stratigraphic boundaries and surface mineralogy. The EMIT Level 2B Mineral Fraction products provide estimated fractional abundances of key rock-forming and alteration minerals at 60-meter spatial resolution, derived via spectral curve fitting against the USGS library. Comparing these abundances with stratigraphic units defined in regional geological maps can be used to test the spectral

consistency of mapped formations. Pixels affected by vegetation or shadow, identified by the EMIT L2B mask, are excluded to isolate the geological surface signal.

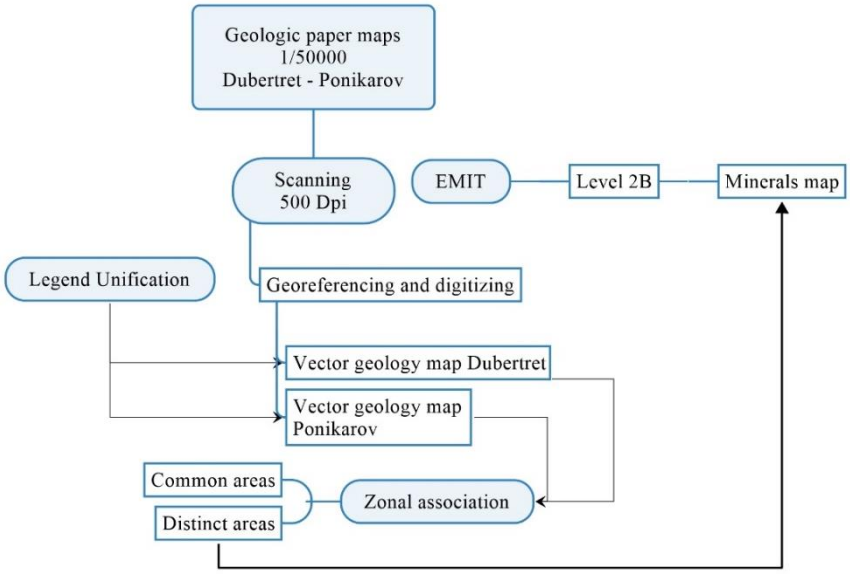

Figure 2: Geoprocessing Workflow for the Comparison of Dubertret and Ponikarov's Geological Maps

The first step in the data preparation and geoprocessing workflow consists of scanning the geological maps at 500 dpi (Figure 1), georeferencing them to the UTM 36N coordinate system, and digitizing them in ArcGIS Pro.

Then the legends are harmonized (Table 1) by standardizing the attribute tables of the vector datasets from Louis Dubertret and Vladimir Ponikarov. A spatial association analysis of their respective geological zones is then performed to establish correspondences between similar units and delineate areas that highlight differences between the two interpretations.

The workflow concludes with a validation step that uses a mineral map derived from EMIT Level 2B hyperspectral imagery. Validation is carried out using zonal statistics on the geological entities and mineral units.

3. Results and Discussions

The Distribution and Area Analysis following the legend unification reveals both similarities and significant structural differences.

Geology Unit	Dubertret (Sq. km)	Ponikarov (Sq. km)	Variance Notes
J4 (M. Jurassic)	53.84 (34.73%)	54.12 (34.92%)	High agreement on regional importance
C2 (U. Aptian)	12.28 (7.93%)	25.28 (16.32%)	Significant discrepancy; Ponikarov maps a larger area
J5 (U. Oxfordian)	4.97 (3.21%)	17.13 (11.05%)	Reflects Ponikarov's higher structural resolution

Table 2: Area Comparison of Digitized Maps

The area calculations show that Jurassic formations are dominant in the study region in both maps. The Middle Jurassic unit J4 accounts for about 35% of the total mapped area in both interpretations (Table 2). This stability indicates that both mapping methods recognize the regional importance of Jurassic carbonate formations in the Anti-Lebanon region. However, Ponikarov's map subdivides the Jurassic formations into more polygons than Dubertret's map, suggesting higher structural resolution. Large differences are seen in the Lower Cretaceous units. The C2 formation is much more prominent on the Ponikarov map than on the Dubertret interpretation. This indicates that a number of the formations identified as C1 by Dubertret were reclassified as C2 in the Soviet mapping. This type of discrepancy is more pronounced along lithologic boundaries, where delineation of stratigraphic contacts is difficult due to structural deformation.

The comparison of the Dubertret and Ponikarov maps shows the evolution of geological mapping strategies in the region (Syria and Lebanon). Dubertret's cartography is a stratigraphic synthesis toward a consistent geological framework. His maps emphasize regional continuity and simplified lithologic boundaries. Ponikarov's work, on the other hand, is an approach to mapping based on structural and engineering considerations. The maps incorporate detailed observations of fractures, faults, and rock mechanical properties, providing higher spatial resolution of geological units. The two mapping traditions are complementary despite their

methodological differences. Stratigraphic nomenclature is largely based on Dubertret's maps, while Ponikarov's maps are a good source of structural information for engineering geology.

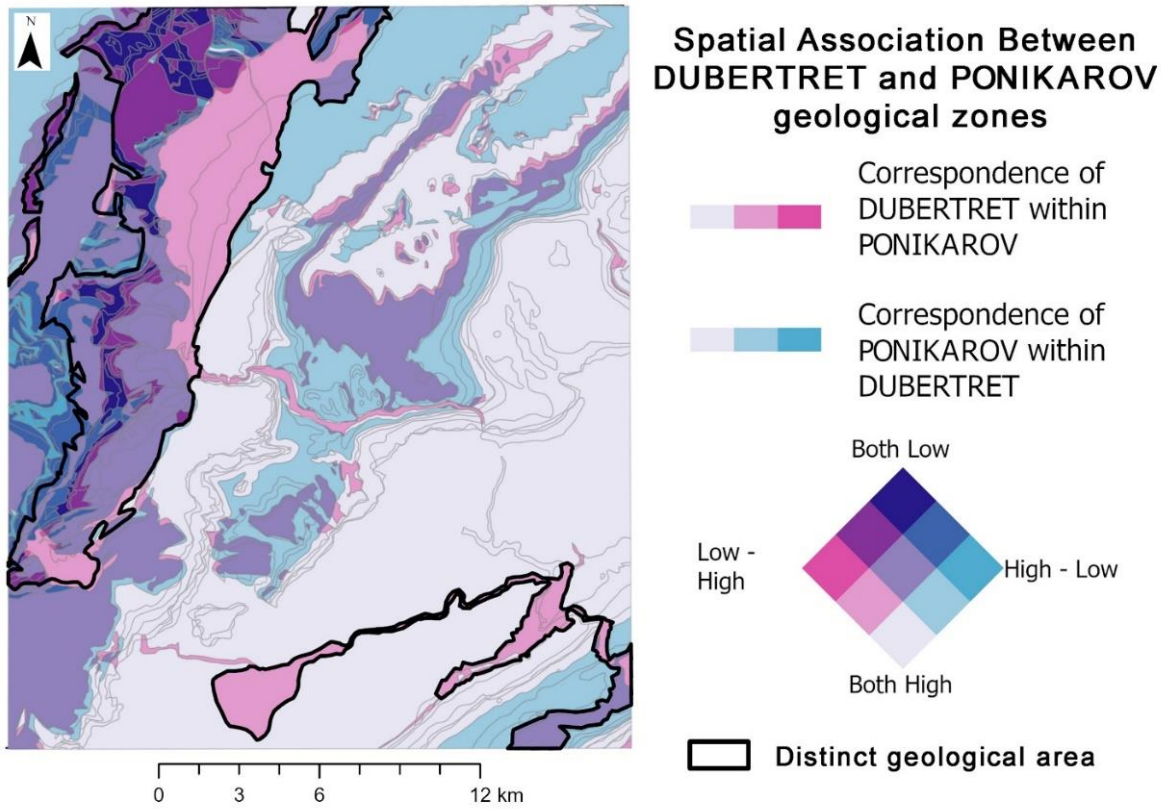

Figure 3: The Map of Spatial Association between Dubertret and Ponikarov Geological Zones

The GIS overlay analysis of the Spatial Association and Disagreement produced a different map (Figure 3) that showed the areas of disagreement between the two geological interpretations. The Zones of Agreement are mainly central carbonate formations, while the Zones of Disagreement, which occupy 20% of the study area, are mainly Lower Cretaceous and Upper Jurassic sequences (Figure 3), a distinct geological area where stratigraphic contacts are ambiguous due to structural deformation. These zones correspond to areas of structural complexity, where geological contacts are equivocal.

Some of the ~20% mismatch between the mapped and spectrally derived lithological units may be due to data masking in the pre-processing step. In the Tetracorder processing chain, pixels affected by vegetation cover, cloud contamination, shadow effects, and low signal-to-noise ratios were excluded prior to spectral matching against the USGS Spectral Library. To evaluate the effect of these exclusions, the total masked area was quantified, showing that a non-negligible proportion of the study area was excluded from spectral classification. The spatial differences observed between the field-based geological map and the remotely sensed mineralogical classification may be explained by the lack of these geological controls, especially in areas with dense vegetation cover or in topographic shadow, where lithological exposure is limited. The high degree of correspondence between Dubertret and Ponikarov indicates that the entities of both maps are very similar in area and geometry. The same pattern is observed for Ponikarov as for Dubertret. The areas of strong correlation are shown in light colors in Figure 3, while the darker shades represent the areas of dissimilarity between the maps. These zones of low correspondence were then characterized and reclassified as discrete geological areas, reflecting the observed variance. Geological maps are often interpolated or drawn at a scale (for example 1:50,000) that smooth out details. The spectral unmixing algorithms applied to EMIT's Level 2B products yield insight into sub-pixel mineral distribution, enabling a more granular assessment of geomorphological features than is typically possible with traditional vector-based geological maps [22,24]. By linking L2B to Geological Maps and applying zonal statistics of the areas of disagreement between Louis Dubertret and Vladimir Ponikarov in ArcGIS Pro, we detected a high concentration of calcite–dolomite mixture (sample AMX8 W1R1Bb) within the Cenomanian and Jurassic units in both maps. The reflectance spectra of mixed calcite–dolomite carbonates in the VNIR–SWIR (0.4–2.5 µm) are characterized by relatively high reflectance overall and diagnostic absorption features controlled by the CO_3^{2-} ion.

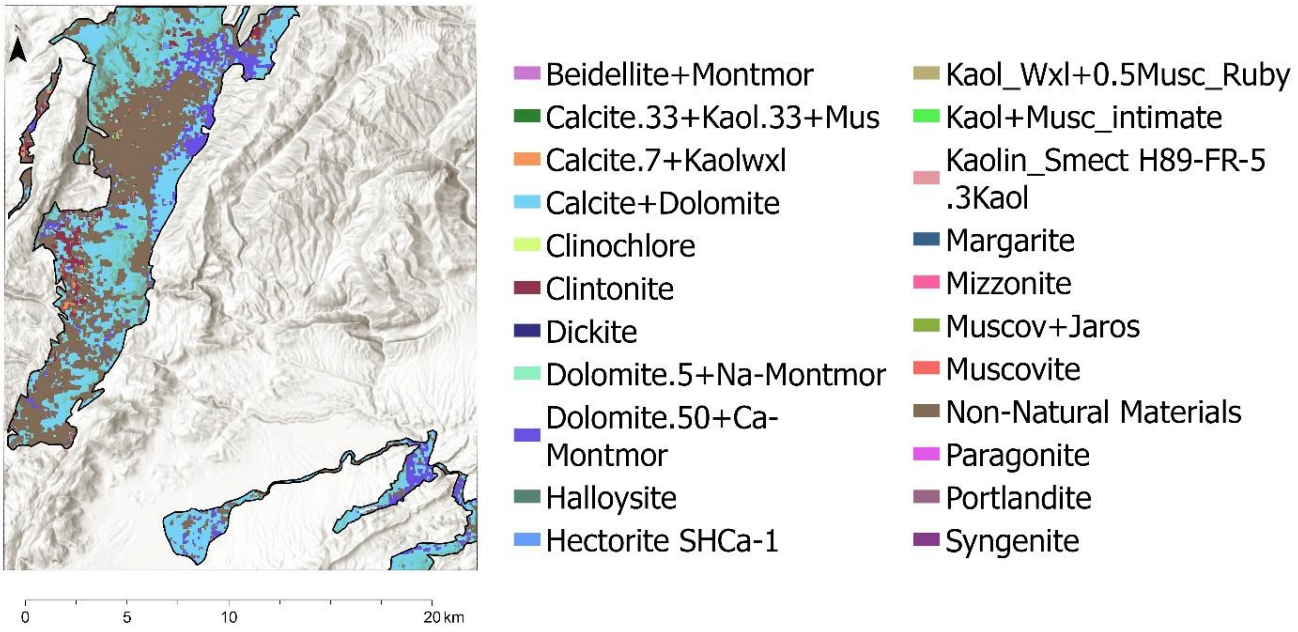

Figure 4: EMIT Minerals Map of the Distinct Area between Dubertret and Ponikarov Geology

The L2B mineral map of the distinct geological region between Dubertret and Ponikarov (Figure 4) revealed the presence of non-natural materials, including fiberglass, plastics, and wood.

In Figure 4, the EMIT mineral map detected non-natural materials such as plastic, fiberglass, and plywood. At that scale, a 60-meter pixel labeled "Plastic" or "Fiberglass" typically indicates greenhouse agriculture (tunnels), localized urban waste, or a spectral misclassification by the automated algorithm.

These were excluded from the analysis, along with vegetative cover such as grass.

The analysis reveals no significant spectral differences between the Dubertret and Ponikarov datasets within the delineated zones of disagreement, as confirmed by spatial association analysis. The primary discrepancy lies in the level of stratigraphic classification detail: Ponikarov subdivides the Cenomanian into six units and the Jurassic into four, whereas Dubertret classifies the Cenomanian into two and the Jurassic into a single unit.

A Validation of Geological Maps Boundaries between the Dubertret and Ponikarov datasets and the L2B data shows the results in Table 3.

Geology	Dubertret	Ponikarov
Bn		Calcite+Dolomite.5 AMX8 W1R1Bb
		Muscovite GDS113 Ruby W1R1Bb splib06 3348
C1		Dickite NMNH106242 W1R1Bb
C2	Calcite+Dolomite.5 AMX8 W1R1Bb	Calcite+Dolomite.5 AMX8 W1R1Bb
	Kaol_Wxl+0.5Musc_Ruby AMX12 W1R1Ba	
C3	Halloysite NMNH106237 W1R1Ha	Halloysite NMNH106237 W1R1Ha
	Calcite+Dolomite.5 AMX8 W1R1Bb	Calcite+Dolomite.5 AMX8 W1R1Bb
	Muscovite GDS113 Ruby W1R1Bb splib06 3348	Clinochlore GDS158 Flagst W1R1Hb
C5		Calcite+Dolomite.5 AMX8 W1R1Bb
		Clinochlore GDS158 Flagst W1R1Hb
C6		Calcite+Dolomite.5 AMX8 W1R1Bb
		Clinochlore GDS158 Flagst W1R1Hb
E		Calcite+Dolomite.5 AMX8 W1R1Bb
J4		Calcite+Dolomite.5 AMX8 W1R1Bb
		Hectorite SHCa-1.Ac-B W1R1Hb

J5	Calcite+Dolomite.5 AMX8 W1R1Bb	Calcite+Dolomite.5 AMX8 W1R1Bb
		Calcite.7+Kaolwxl.3 AMX9 W1R1Ba
J6		Calcite+Dolomite.5 AMX8 W1R1Bb
		Halloysite NMNH106237 W1R1Ha
J7		Halloysite NMNH106237 W1R1Ha
N1		Calcite+Dolomite.5 AMX8 W1R1Bb
		Muscovite GDS113 Ruby W1R1Bb splib06 3348
N2		Calcite+Dolomite.5 AMX8 W1R1Bb
		Muscovite GDS113 Ruby W1R1Bb splib06 3348
q		Calcite+Dolomite.5 AMX8 W1R1Bb

Table 3: EMIT Minerals Spectral Signatures Found in Dubertret And Ponikarov Geological Entities

As shown in Table 3, although both maps capture the general "skeleton" of the region, Ponikarov's mapping (probably due to its higher resolution or different field methodology) reveals a much more complex mineralogical diversity when validated against EMIT's spectral signatures.

There is a high agreement for the Lower and Middle Cretaceous (C2) and (C3). Both maps are consistent with a Calcite + Dolomite signature. Both interpretations validate C2 as a coherent, massive carbonate platform. Both mention Halloysite (a clay mineral). Thus, C3 seems to be a reliable marker bed of marly or argillaceous material, readily recognizable by its spectral "dip" at ~2.2 micrometers [24,25].

A telling scientific difference emerges in the more detailed analysis of unit C3: Muscovite (Al-rich mica) is shown in the mapped area of Dubertret. Clinochlore (Mg-Fe-rich chlorite) is shown in the mapped area of Ponikarov. This means that Ponikarov was able to differentiate between types of pelitic (clay-rich) facies. Muscovite often suggests a more terrestrial/detrital source, whereas Clinochlore may indicate low-grade metamorphism, or more likely in this context, weathering of volcanic interbeds common in the Syrian Cretaceous sequence [26,27].

The data indicate that the map units of Ponikarov (Bn, C1, C5, C6, E, J, N) relate to a variety of specialized minerals that are absent in the Dubertret data points: Dickite (Unit C1): High temperature polymorph of Kaolinite [28,29]. Its occurrence in C1 (but not in others) suggests that the C1 unit of Ponikarov may be following a particular hydrothermal or deep-weathering zone not captured in the broader classification of Dubertret [30,31]. Hectorite (transition from Unit J4/J5): A rare Mg-rich smectite clay [32,33]. Its occurrence within the Jurassic sequence (J) is significant – typically it is indicative of alkaline lacustrine environments or altered volcanic ash. [27,34].

Feature	Dubertret Performance	Ponikarov Performance	EMIT Validation Note
Carbonate Detection	High (C2, J5)	High (Multiple Units)	Both maps accurately identify the limestone/ dolomite "backbone."
Clay Differentiation	General (Halloysite)	Specific (Dickite, Hectorite, Halloysite)	Ponikarov aligns better with the terrain's hyperspectral diversity.
Spectral Coverage	Sparse	Dense/Comprehensive	Ponikarov's units appear to be more spatially precise relative to the EMIT pixels.

Table 4: A Summary of the Geological Maps Validation with EMIT

The Ponikarov map appears to be a more "sensitive" tool for the Zabadani area than the EMIT data. Dubertret correctly identified the major stratigraphic breaks (the "macro" view), while Ponikarov captured the mineralogical transitions (the "micro" view) within the Cretaceous and Jurassic layers. The EMIT data show that Muscovite, Clinochlore, and Hectorite are present in the geology of Zabadani, which is not simply "limestone" but a complex combination of carbonates and phyllosilicates. If you are doing further work, I suggest using the Ponikarov boundaries as your main baseline, as they correlate better with the real surface mineralogy detected from space.

The Jurassic section in the Zabadani region (J4 to J7) is highly informative, as it represents a transition from massive, "clean" marine carbonates to more complex, "dirty" sediments containing clay minerals.

When we look at the Ponikarov data points in sequence, we see a clear mineralogical evolution with:

- J4: Hectorite (Mg-Smectite)
- J5 : Calcite + Dolomite (Pure Carbonate)

- J6/J7: Halloysite (Al-Silicate Clay)

This is not random. The Late Jurassic in the Anti-Lebanon range is characterized by a "shallowing-upward" sequence [35,36]. The environmental shift from deep-water carbonate platforms (J5) to lagoonal or nearshore settings (J6/J7), where terrestrial clays (such as Halloysite) could wash in was driven by either a lowering of sea level or a rise in land elevation [36,37]. Dubertret may have mapped J6 as limestone because it resembles weathered limestone in the field. EMIT, however, "sees" through the visual appearance and identifies the Al-OH absorption feature at 2.2 micrometers.

Halloysite usually forms by weathering of aluminosilicate minerals [38,39]. This indicates that these Jurassic units are more marly (clay-rich) than previously thought [40,41]. Halloysite is observed in J7, confirming the transition to the "Basal Sands" or "Lower Cretaceous Clastics" (C1) with a dominant terrestrial influence [42,43]. The EMIT sensor detected Hectorite in J4. Hectorite is a magnesium-rich clay closely associated with altered volcanic ash (bentonite) or very specific alkaline lake environments [44,45]. This suggests that Ponikarov's J4 unit may contain thin volcanic interbeds or tuffaceous material that was not recognized during previous mapping but was identified in hyperspectral validation [46,47]. The difference between the maps is essentially a facies resolution: • Dubertret mapped lithostratigraphy (what the rock looks like). • Ponikarov + EMIT are mapping the "Chemostratigraphy" (what the rock is made of). The transition from Halloysite (Upper Jurassic: J6/J7) to Hectorite (Lower Jurassic: J4) indicates that the Zabadani area has undergone significant environmental fluctuations (volcanism and sea-level changes). Ponikarov's map captured these spatial variations more effectively, despite not having the mineral names in hyperspectral data at the time.

4. Conclusion

A digital synthesis of the 1:50,000-scale geological maps of the Zabadani region by Louis Dubertret and Vladimir Ponikarov shows that historical cartographic frameworks can be complementary rather than contradictory. Dubertret's work provides robust regional stratigraphy and nomenclature, while Ponikarov's structural maps reveal fine lithofacies differences that correlate with spaceborne hyperspectral data. Validation with mineral-fraction data from EMIT Level 2B confirms the major carbonate zones and highlights localized clay and alteration facies, including halloysite, clinochlore, hectorite, dickite, and muscovite, which help resolve spatial discrepancies among the original authors. In his stratigraphic subdivisions of the Cenomanian and Jurassic strata into finer units, Ponikarov often found that EMIT data showed distinct mineral trends. This indicates that the differences between the maps are lithologic or diagenetic rather than errors. Our GIS-based approach reveals areas of cartographic divergence across 20% of the landscape, where field re-surveys and stratigraphic updates are most needed. For practical purposes, Ponikarov's limits are a better basis for engineering, mineral exploration, and hydrogeological modeling. Dubertret's nomenclature remains the standard for regional overviews. Next steps include targeted field sampling and spectroscopy to confirm minerals identified from satellite data, assess the effects of surface cover on spectral data, and apply machine-learning tools to historical and spectral datasets to build a modern, multi-source geological database for the Zabadani basin [48-51].

References

1. Smith, D., Johnson, R., Lee, M. (2010). The Role of Geological Mapping in Tectonically Complex Regions. *Journal of Structural Geology, 32*(8), 1010–1025.
2. Jones, P., Brown, S. (2015). Principles of Geological Mapping and Spatial Analysis. *Earth-Science Reviews, 150*, 1–25.
3. Dubertret, L. (1953). Geological Map of Lebanon and Syria. *French Geological Survey*.
4. Ponikarov, V. P. (1960). Geological Maps of Syria: Structural and Lithomechanical Analysis. *Soviet Geological Society Bulletin,* 12(3), 45–78.
5. Dubertret, L., Chabard, J. (1960). Stratigraphic Synthesis of Lebanon. *Bulletin De La Societe Geologique De France, 5*(1), 25–58.
6. Ivanov, V., Petrov, A., Smirnov, Y. (1975). Soviet Geological Surveys in Syria: Structural Mapping Approaches. Moscow University Press.
7. Al-Hussain, A., Kher, I., Mahfouz, M. (2008). Structural Analysis and Geological Mapping in the Levant Region. *Geological Journal, 43*(2), 101–115.
8. Ariza-Lopez, F., Perez-Rodriguez, R., Garcia, M. (2010). Integration of Historical Geological Maps into Gis for Spatial Analysis. *Computers & Geosciences, 36*(7), 911–921.
9. Sabins Jr, F. F., & Ellis, J. M. (2020). Remote sensing: Principles, interpretation, and applications. Waveland Press.
10. Droubi, A., Al-Sibai, M., Abdallah, A., Zahra, S., Obeissi, M., Wolfer, J., ... & Schelkes, K. (2008). A decision support system (DSS) for water resources management,–Design and results from a pilot study in Syria. In Climatic changes and water resources in the Middle East and North Africa (pp. 199-225). Berlin, Heidelberg: Springer Berlin Heidelberg.
11. Dubertret, L. (1951). République Syrienne: Carte Géologique au 1/50 000, Feuille de Zebdani. *Geological Magazine, 88*(3), 220.
12. The Arab Center for the Studies of Arid Zones and Dry Lands (ACSAD), & Federal Institute for Geosciences and Natural Resources (BGR). (2007). *Decision support system for the Zabadani Basin: Management, protection, and sustainable use of groundwater and soil resources*.
13. Asfahani, J. (2013). Groundwater potential estimation using vertical electrical sounding measurements in the semi-arid Khanasser Valley region, Syria. *Hydrological sciences journal, 58*(2), 468-482.
14. Al-Hilal, M. (2016). Establishing the Range of Background for Radon Variations in Groundwater along the Serghaya Fault in Southwestern Syria. Geofísica internacional, 55(4), 255-266.
15. United Nations Economic and Social Commission for Western

Asia (ESCWA), & Bundesanstalt für Geowissenschaften und Rohstoffe (BGR). (2013). Anti-Lebanon. In *Inventory of shared water resources in Western Asia*. ESCWA.
16. Gillespie, A. R., Hoekzema, R., O'Neill, J. (2005). Remote Sensing and Gis in Geological Mapping. *International Journal of Remote Sensing, 26*(10), 2031–2054.
17. Bonham-Carter, G. (1994). *Geographic information systems for geoscientists: modelling with GIS* (No. 13). Elsevier.
18. Richards, J. A., & Jia, X. (2006). Interpretation of hyperspectral image data. In *Remote sensing digital image analysis: An introduction* (pp. 313-337). Berlin, Heidelberg: Springer Berlin Heidelberg.
19. Camps-Valls, G., Tuia, D., Bruzzone, L., & Benediktsson, J. A. (2013). Advances in hyperspectral image classification: Earth monitoring with statistical learning methods. *IEEE signal processing magazine, 31*(1), 45-54.
20. Green, R. O., Mahowald, N., Ung, C., Thompson, D. R., Bator, L., Bennet, M., ... & Zan, J. (2020, March). The Earth surface mineral dust source investigation: An Earth science imaging spectroscopy mission. In *2020 IEEE aerospace conference* (pp. 1-15). IEEE.
21. Li, L., Mahowald, N. M., Miller, R. L., Pérez García-Pando, C., Klose, M., Hamilton, D. S., ... & Thompson, D. R. (2020). Quantifying the range of the dust direct radiative effect due to source mineralogy uncertainty. *Atmospheric Chemistry and Physics Discussions, 2020*, 1-58.
22. Thompson, D. R., Green, R. O., Bradley, C., Brodrick, P. G., Mahowald, N., Dor, E. B., ... & Zandbergen, S. (2024). On-orbit calibration and performance of the EMIT imaging spectrometer. *Remote Sensing of Environment, 303,* 113986.
23. NASA Jet Propulsion Laboratory. (2022). *EMIT Level 2A estimated surface reflectance and uncertainty and masks V001* [Data set]. LP DAAC.
24. Abrams, M. J., Goetz, A. F., & Lang, H. (1983). New techniques for clay mineral identification by remote sensing. AAPG Bulletin, 67(3), 410-410.
25. Bishop, J. L., Lane, M. D., Dyar, M. D., & Brown, A. J. (2008). Reflectance and emission spectroscopy study of four groups of phyllosilicates: Smectites, kaolinite-serpentines, chlorites and micas. *Clay minerals, 43*(1), 35-54.
26. Wells, M., Morton, A., & Frei, D. (2017). Provenance of Lower Cretaceous clastic reservoirs in the Middle East. *Journal of the Geological Society, 174*(6), 1048-1061.
27. Al-Riyami, K., & Robertson, A. (2002). Mesozoic sedimentary and magmatic evolution of the Arabian continental margin, northern Syria: evidence from the Baer–Bassit Melange. *Geological magazine, 139*(4), 395-420.
28. Palinkaš, S. S., Šoštarić, S. B., Bermanec, V., Palinkaš, L., Prochaska, W., Furić, K., & Smajlović, J. (2009). Dickite and kaolinite in the Pb-Zn-Ag sulphide deposits of northern Kosovo (Trepča and Crnac). *Clay minerals, 44*(1), 67-79.
29. Schroeder, R. J., & Hayes, J. B. (1968). Dickite and kaolinite in Pennsylvanian limestones of southeastern Kansas. *Clays and Clay Minerals, 16*(1), 41-49.
30. Çelik, M., Karakaya, N., & Temel, A. (1999). Clay minerals in hydrothermally altered volcanic rocks, Eastern Pontides, Turkey. *Clays and Clay Minerals, 47*(6), 708-717.
31. Nayebi, N., Raeisi, D., Fallahi, H., Babazadeh, S., & Modabberi, S. (2026). Integrated VNIR–SWIR Spectral, Mineralogical, and Geochemical Classification of Hydrothermal Alteration Zones in the Shadan Au–Cu System, Eastern Iran. *Minerals, 16*(4), 379.
32. Christidis, G. E., Aldana, C., Chryssikos, G. D., Gionis, V., Kalo, H., Stöter, M., ... & Robert, J. L. (2018). The nature of laponite: pure hectorite or a mixture of different trioctahedral phases?. *Minerals, 8*(8), 314.
33. Zhang, J., Zhou, C. H., Petit, S., & Zhang, H. (2019). Hectorite: Synthesis, modification, assembly and applications. *Applied Clay Science, 177,* 114-138.
34. Andrews, J. E. (1987). Jurassic clay mineral assemblages and their post-depositional alteration: Upper Great Estuarine Group, Scotland. *Geological Magazine, 124*(3), 261-271.
35. Clark, N., & BouDagher-Fadel, M. (2004). Larger benthic foraminifera and calcareous algae of the Upper Kesrouane Limestone Formation (Middle/Upper Jurassic) in Central Lebanon: stratigraphy, sedimentology and regional synopsis. Revue de Paléobiologie, 23, 475-504.
36. Collin, P. Y., Mancinelli, A., Chiocchini, M., Mroueh, M., Hamdam, W., & Higazi, F. (2010). Middle and Upper Jurassic stratigraphy and sedimentary evolution of Lebanon (Levantine margin): palaeoenvironmental and geodynamic implications.
37. Haq, B. U. (2018). Jurassic sea-level variations: a reappraisal. *GSA today, 28*(1), 4-10.
38. Bates, T. F. (1962). Halloysite and gibbsite formation in Hawaii. In *Clays and Clay Minerals* (pp. 315-328). Pergamon.
39. Keeling, J. L., Pasbakhsh, P., & Churchman, G. J. (2015). The mineralogy, geology and occurrences of halloysite. *Natural Mineral Nanotubes,* 95-115.
40. Hirsch, F., & Picard, L. (1988). The Jurassic facies in the Levant. *Journal of Petroleum Geology, 11*(3), 277-308.
41. Abdel-Rahman, A. F., & Nader, F. H. (2002). Characterization of the Lebanese Jurassic–Cretaceous carbonate stratigraphic sequence: a geochemical approach. *Geological journal, 37*(1), 69-91.
42. Bentor, Y. K., Bodenheimer, W., & Heller, L. (1963). A reconnaissance survey of the relationship between clay mineralogy and geological environment in the Negev (southern Israel). *Journal of Sedimentary Research, 33*(4), 874-903.
43. Ferry, S., Merran, Y., Grosheny, D., & Mroueh, M. (2007). The Cretaceous of Lebanon in the Middle East (levant) context. *Carnets de Géologie/Notebooks on Geology*, (M02/08), 38-42.
44. Ames, L. L., Sand, L. B., & Goldich, S. S. (1958). A contribution on the Hector, California, bentonite deposit. *Economic Geology, 53*(1), 22–37.
45. Starkey, H. C., & Blackmon, P. D. (1979). *Clay mineralogy of Pleistocene Lake Tecopa, Inyo County, California* (No. 1061). US Govt. Print. Off.,.
46. Farrand, W. H. (1991). Visible and near-infrared reflectance of

tuff rings and tuff cones. The University of Arizona.
47. Corrado, F., Putzolu, F., Armstrong, R. N., Mondillo, N., Chirico, R., Casarotto, B., ... & Herrington, R. J. (2025). Application of satellite and proximal hyperspectral sensing to target lithium mineralization in volcano-sedimentary deposits: A case study from the McDermitt caldera, USA. *Remote Sensing of Environment, 323*, 114724.
48. Dubertret, L. (1955). Carte Géologique du Liban. Ministère des Travaux Publics.
49. Droubi, A., Al-Sibai, M., Abdallah, A., Zahra, S., Obeissi, M., Wolfer, J., ... & Schelkes, K. (2008). A decision support system (DSS) for water resources management,–Design and results from a pilot study in Syria. In *Climatic changes and water resources in the Middle East and North Africa* (pp. 199-225). Berlin, Heidelberg: Springer Berlin Heidelberg.
50. Nader, F. H. (2014). The Geology of Lebanon. Springer.
51. Ponikarov, V. P. (1967). The Geology of Syria: Explanatory Notes on the Map of Syria, Scale 1:500,000. Part ii: Mineral Deposits and Underground Water Resources. Technoexport.